

RESEARCH ARTICLE

Characterisation of extracellular vesicles in baculovirus infection of *Spodoptera frugiperda* cells

Lex J. C. Van Es^{1,2}  | Robert D. Possee² | Linda A. King¹¹Department of Biological and Medical Sciences, Oxford Brookes University, Oxford, UK²Oxford Expression Technologies Ltd, Oxford, UK**Correspondence**Linda King, Department of Biological and Medical Sciences, Oxford Brookes University, Oxford, OX3 0BP, UK. Email: laking@brookes.ac.uk**Funding information**

Oxford Expression Technologies Ltd.; Oxford Brookes University

Abstract

Autographa californica multiple nucleopolyhedrovirus (AcMNPV) is an enveloped DNA virus of the *Baculoviridae* family. This baculovirus is widely exploited for the biological control of insect pest species and as an expression platform to produce recombinant proteins in insect cells. Extracellular vesicles (EVs) are secreted by all cells and are involved in key roles in many biological processes through their cargo consisting of proteins, RNA or DNA. In viral infections, EVs have been found to transfer both viral and cellular cargo that can elicit either a pro- or antiviral response in recipient cells. Here, small EVs (sEVs) released by *Spodoptera frugiperda* (Sf) insect cells were characterised for the first time. Using *S. frugiperda* (SfC1B5) cells stably expressing the baculovirus *gp64*, the viral envelope protein GP64 was shown to be incorporated into sEVs. Sf9 cells were also transfected with a bacmid AcMNPV genome lacking *p6.9* (AcΔP6.9) to prevent budded virus production. The protein content of sEVs from both mock- and AcΔP6.9-transfected cells were analysed by mass spectrometry. In addition to GP64, viral proteins Ac-F, ME-53 and viral ubiquitin were identified, as well as many host proteins including TSG101—which may be useful as a protein marker for sEVs.

KEYWORDSAcMNPV, baculovirus, extracellular vesicles, GP64, insect, P6.9, proteomics, *Spodoptera frugiperda*, virus

1 | INTRODUCTION

Baculoviruses infect Diptera, Hymenoptera and Lepidoptera insects and are commonly used for the biological control of crops damaged by these insects (Harrison et al., 2018). The baculovirus *Autographa californica* multiple nucleopolyhedrovirus (AcMNPV)—recently renamed as *Alphabaculovirus aualifornicae* (<https://ictv.global/taxonomy/>)—is also widely used for protein manufacture, using *Spodoptera frugiperda* (Sf) or *Trichoplusia ni* cells as a production platform. It contains a 134 kb DNA genome (Ayres et al., 1994) and produces two types of virions: occlusion-derived virus, which is occluded into proteinaceous bodies called polyhedra and infects new larval hosts; and budded virus (BV), which mediates cell to cell spread within the host, and in cell culture. The BV exits the host cell through the plasma membrane, where it acquires an envelope containing the viral glycoprotein GP64 (Volkman et al., 1984). An essential protein for the formation of BV is P6.9, which condenses the DNA genome; without P6.9 no BV are formed (Wang et al., 2010a).

1.1 | Extracellular vesicles

Cells produce and secrete nanoparticles called extracellular vesicles (EVs). There are three types of EVs based on origin: exosomes, microvesicles (MVs) and apoptotic vesicles (Colombo et al., 2014). The latter type is formed when a cell dies through

This is an open access article under the terms of the [Creative Commons Attribution-NonCommercial](https://creativecommons.org/licenses/by-nc/4.0/) License, which permits use, distribution and reproduction in any medium, provided the original work is properly cited and is not used for commercial purposes.

© 2024 The Author(s). *Journal of Extracellular Biology* published by Wiley Periodicals LLC on behalf of International Society for Extracellular Vesicles.

apoptosis, while MVs are vesicles that bud off directly from the plasma membrane of the cell (Atkin-Smith et al., 2015; Heijnen et al., 1999). Finally, exosomes are formed by inward budding into an early endosome, at which point the vesicles are termed intraluminal vesicles (ILVs) (Gruenberg, 2020). With numerous of these ILVs inside, the early endosome becomes a multivesicular body (MVB). This MVB might fuse with a lysosome to degrade its content (Gruenberg, 2020). Alternatively, it can fuse with the plasma membrane, releasing its content including the ILVs into the extracellular milieu, at which point the ILVs become exosomes (Gruenberg, 2020; Perrin et al., 2021).

Approximately, exosomes are 30–150 nm, MVs are 100–1000 nm and apoptotic bodies are 1–5 μ M (Atkin-Smith et al., 2015; Colombo et al., 2014). Nevertheless, within these size ranges mixed populations exist; for example, mixed populations of exosomes and microvesicles have been described (Kowal et al., 2016; Tauro et al., 2012). Therefore, isolated EVs are generally referred to by size or density, for example, small EVs (sEVs) instead of exosomes (Théry et al., 2018). While characterisation of EVs has mainly focused on those secreted by mammalian cells, EVs are secreted by all cells. Therefore, it is likely that conserved biogenesis pathways exist, and while the precise cargo may differ, EVs of *S. frugiperda* can be expected to contain homologs of tetraspanins, components of the endosomal sorting complex required for transport (ESCRT) and other proteins involved in their biogenesis. Indeed, proteomics identified similar proteins enriched in EVs of insect model organism *Drosophila melanogaster*, such as small GTPases, heat shock proteins and a tetraspanin (Koles et al., 2012; Koppen et al., 2011; Parchure et al., 2015).

1.2 | Extracellular vesicles in viral infections

Viruses can dramatically alter cellular processes, and influence the content of EVs, as observed for the human immunodeficiency virus type 1 (HIV-1) virus, among others (Alem et al., 2021; Booth et al., 2006; Campbell et al., 2008; Dogrammatzis et al., 2021; Martin-Jaular et al., 2021). Extracellular vesicles of HIV-1-infected cells were reported to contain functional RNA and proteins, and cells pre-treated with these EVs were more susceptible to HIV-1 infection (Boucher et al., 2023; Cho et al., 2021). Similar results were found for other human viruses such as dengue virus (Reyes-Ruiz et al., 2019), Epstein-Barr virus (Sato et al., 2022), herpes simplex virus 1 (Dogrammatzis et al., 2021) and Rift Valley fever virus (Alem et al., 2021). Interestingly, EVs were found to elicit both proviral responses (Martínez-Rojas et al., 2020; Reyes-Ruiz et al., 2019; Sato et al., 2022) and antiviral responses (Alem et al., 2021; Tassetto et al., 2017). Moreover, for the herpes simplex virus 1, EVs both beneficial and detrimental to infectivity were purified (Dogrammatzis et al., 2021). This was possible due to the heterogeneous nature of EVs.

The role of EVs in the interaction between a human virus and the insect vector has also been studied. When ticks feed on their host, they release EVs in their saliva (Oliva Chávez et al., 2021; Zhou et al., 2020). These EVs can suppress the immune system in their mammalian hosts (Oliva Chávez et al., 2021), via transmission of miRNAs (Hackenberg et al., 2017). This is important to the ticks for their feeding success but could benefit the transfer of virus from the tick saliva to the host, as was reported for bacteria (Oliva Chávez et al., 2021). For the Zika virus, it was discovered that infected mosquito cells produce EVs that contain the viral envelope protein and carry viral RNA (Martínez-Rojas et al., 2020). Moreover, these EVs released by infected mosquito cells alone were sufficient to infect mosquito and mammalian cells (Martínez-Rojas et al., 2020). They also aid infection of mammalian cells by stimulating a pro-inflammatory immune response of monocytes (Martínez-Rojas et al., 2020).

Most studies on EVs in viral infection have focused either on human cells or on insect vectors of human viruses such as ticks and mosquitos. Though the presence of EVs has been described in *S. frugiperda* cells, little research has been performed on the role they may play in baculovirus infection (Hashimoto et al., 2017; Hodgson et al., 2022; Ishikawa et al., 2020; Puente-Massaguer et al., 2022). Recently, sEVs were characterised by mass spectrometry in AcMNPV-infected *T. ni* cells, although the presence of viral proteins was not evaluated since no full separation of sEVs from BV was achieved (Hausjell et al., 2023). Here, sEVs were characterised from both uninfected and baculovirus-infected *S. frugiperda* cells. Similar to Hausjell et al. (2023), attempts to characterise sEVs from baculovirus-infected cells proved challenging as BV co-purified with sEVs. In this study, this was overcome by characterising sEVs from a stable cell line expressing *gp64*, and by transfecting cells with an AcMNPV bacmid lacking *p6.9* (Ac Δ P6.9), which produced no BV. In both cases, the baculovirus glycoprotein GP64 was found to be incorporated into sEVs. The protein content of sEVs from Sf9 cells transfected with Ac Δ P6.9 was analysed by mass spectrometry.

2 | MATERIALS AND METHODS

2.1 | Cell culture

S. frugiperda (Sf9) cells (Thermo Fisher Scientific, USA) were cultured in suspension in shake flasks at 28°C in ESF-921 media (Expression Systems, USA). SfCIB5 (Oxford Expression Technologies Ltd., UK), a clonal derivative of Sf21 cells (Vaughn et al., 1977), and SfCIB5-GP64 cells were cultured in ESF-AF media (Expression Systems, USA).

2.2 | Generating a stable cell line expressing gp64

The pIEK1-*neo*_OpIE2-gp64 plasmid was generated by inserting the AcMNPV immediate early promoter (Ac-IE-01) expressing a kanamycin/neomycin resistance gene (*neo*), and the *Orgyia pseudotsugata* multiple nucleopolyhedrovirus (OpMNPV) immediate early promoter (OpIE-2) into pT7T3-18U (Addgene, USA). The AcMNPV gp64 coding region was then inserted downstream of the OpIE-2 promoter (Figure S1). The pIEK1-*neo*_OpIE2-gp64 plasmid was sequenced to confirm the absence of mutations prior to use in further experiments. SfC1B5 cells were seeded in a 12-well plate at 0.4×10^6 cells per well and transfected with 500 ng plasmid pIEK1-*neo*_OpIE2-gp64. The following day 600 $\mu\text{g}/\text{mL}$ geneticin (Gibco, USA) was added to the medium to select for transfected cells. Once confluent, cells were subcultured initially in monolayer cultures and then expanded to shake cultures without geneticin. The presence of gp64 was confirmed by PCR (Figure S2) and by small scale expression studies.

2.3 | Virus and bacmid

For baculovirus infections, the C6 strain of wild-type (WT) AcMNPV was used (Possee, 1986; Possee et al., 1991). The Ac Δ p6.9 bacmid was created by replacing the p6.9 gene with a kanamycin/neomycin resistance gene (*neo*) (Figure S3). *Escherichia coli* were used that harboured an AcMNPV bacmid with a replicon and a chloramphenicol resistance gene (*chlR*) at the polyhedrin locus. These were transfected with a construct containing *neo* flanked by two regions homologous to DNA both sides of the p6.9 gene in the bacmid. Modified bacmids were selected by plating transformed *E. coli* on plates with kanamycin.

2.4 | Extracellular vesicle isolation

Culture medium was clarified at $300 \times g$ for 5 min to pellet cells, then further clarified at $16,500 \times g$ at 4°C for 20 min. Following concentration to 0.5 mL in a Vivaspin 20 100k MWCO column (Sigma-Aldrich, USA; $3000 \times g$ at 4°C), the concentrated sample was further purified by size exclusion chromatography (SEC). The SEC columns were prepared with Sepharose CL-2B (Cytiva Life Sciences, USA) in a 20 mL column, and washed three times with PBS prior to use. The 0.5 mL concentrated sample was run through the SEC column, using PBS for the liquid phase. Fifteen 0.5 mL fractions were collected and analysed for particle concentration by nanoparticle tracking analysis (NTA) and protein quantification by Pierce BCA protein assay kit (Thermo Fisher Scientific, USA) according to the manufacturer's instructions. Based on initial results, fractions 6–10 were pooled and concentrated to approximately 200 μL , using Vivaspin 2 100k MWCO columns (Sigma-Aldrich, USA; $3000 \times g$ at 4°C).

2.5 | Nanoparticle tracking analysis (NTA)

The particle count of the SEC fractions was determined by NTA using a ZetaView® (Particle Metrix, Germany). Calibration was performed with 100 nm beads. The acquisition settings used were a shutter speed of 100, sensitivity of 80 and 30 frames per second, at room temperature. Each sample was diluted 1:1000 in PBS prior to loading into the machine. Quantity and size were calculated by the software for 11 positions.

2.6 | Transmission electron microscopy (TEM)

For TEM, samples were prepared on a carbon-coated formvar grid, 300 mesh (Taab, UK). The grids were activated by glow discharge using a Turbo Carbon Coater (Agar Scientific, UK). Samples (10 μL) were incubated on the grids for at least 2 min. The grids were then stained with 2% uranyl acetate for 10 s. The grids were left to dry before imaging them on the JEM-1400 Flash (Jeol, Japan) at 120 kV with a Gatan OneView 16 Megapixel camera.

2.7 | Immunogold transmission electron microscopy

Samples were prepared on a carbon-coated formvar grid, 300 mesh (Taab, UK). The grids were activated by glow discharge using a Turbo Carbon Coater (Agar Scientific, UK). Samples (10 μL) were incubated on the grids for at least 2 min, then the grid was blocked with PBS-BSA (1%) for 30 min. Primary anti-GP64 AcV1 (Santa Cruz Biotechnology, USA; diluted 1:50) in PBS-BSA (1%) was applied for 1 h. The grids were washed three times in PBS-BSA (1%) and secondary anti-mouse-gold 10 nm (Sigma-Aldrich, USA; diluted 1:50) was applied for 1 h. The grids were washed three times in PBS, and then fixed in 2.5% glutaraldehyde

for 10 min. The grids were washed three times in Milli-Q water and stained with 2% uranyl acetate for 10 s. The grids were left to dry before imaging them on the JEM-1400 Flash (Jeol, Japan) at 120 kV with a Gatan OneView 16 Megapixel camera.

2.8 | SDS-PAGE, Western blot

SDS-PAGE and Western blot were performed using standard methods (Sambrook & Russell, 2001). The prepared samples were run on a 12% SDS-PAGE gel. After transfer to a nitrocellulose membrane, proteins were stained with Revert total protein stain (Li-Cor, USA), following the manufacturer's instructions. Membranes were probed with a primary anti-GP64 AcV5 antibody (Sigma-Aldrich, USA; diluted 1:2800) and a secondary goat anti-mouse antibody (Sigma-Aldrich, USA, diluted 1:50,000). GP64 was visualised by ECL (Bio-Rad AbD Serotec, USA) and imaged using the ChemiDoc imaging system (Bio-Rad AbD Serotec, USA).

2.9 | Transfection of Sf9 cells with AcΔP6.9

Sf9 cells in suspension culture were transfected with AcΔP6.9 bacmid. Cells were seeded at 0.8×10^6 cells/mL and transfected with 500 ng bacmid DNA using 1.2 μL BaculoFectinII (Oxford Expression Technologies Ltd., UK) and 100 μL TC100 media (Gibco, USA), per mL of cells. A mock mixture was prepared by omitting the bacmid DNA. The mixtures were incubated at room temperature for 15–20 min before being added to the suspension cultures. The cells were incubated on a shaking platform at 28°C and sEVs were harvested at one day post-transfection.

2.10 | Flow cytometry

Transfection efficiency was analysed by flow cytometry, for which a protocol by Mulvanian et al. (2004) had been adapted by Dr. L.P. Graves (personal communication, 2021). Per shake flask, three 500 μL aliquots were collected and cells were pelleted at 4000 rpm for 5 min. The pellet was washed in 100 μL dPBS and pelleted again at 4000 rpm for 5 min. The pellet was then resuspended in 100 μL dPBS-BSA (1%) with anti-GP64-APC (Invitrogen, USA; diluted 1:1000) and incubated on ice in the dark for 1 h. The cells were pelleted at 4000 rpm for 5 min and washed once in 100 μL dPBS. After pelleting, the cells were resuspended in 100 μL dPBS and dispensed into a 96-well plate. The transfection efficiency was then assessed using the NovoCyte NovoSampler Pro (ACEA Biosciences Inc. USA).

2.11 | Mass spectrometry

Small EVs were lysed using RIPA lysis buffer (10×; Merck Millipore, Germany) and protease inhibitor cocktail (set III, EDTA free; Merck Millipore, Germany). This mixture was incubated on ice for 3 h to allow lysis. The proteins (33 μg per sample) were then digested with trypsin using the FASP kit (Abcam, UK) according to the manufacturer's instructions. Following elution, the peptides were freeze-dried in a ScanVac Coolsafe freeze dryer (Labogene, Denmark) until all ice had sublimated. The peptides were then sent to the University of Birmingham (School of Biosciences) for identification via mass spectrometry (MS).

Peptides were concentrated and separated using the UltiMate[®] 3000 high-performance liquid chromatography (HPLC) series (Dionex, Sunnyvale, CA USA). The samples were then trapped on a precolumn (Acclaim[™] PepMap[™] 100 C18 HPLC Column, 3 μm, 75 μm internal diameter × 150 mm; Thermo Fisher Scientific) and separated in Nano Series[™] Standard Columns 75 μm internal diameter × 15 cm, packed with C18 PepMap100, 3 μm, 100 Å (Dionex, Sunnyvale, CA USA). The gradient used ranged from 3.2% to 44% solvent B (0.1% formic acid in acetonitrile) diluted with solvent A (0.1% formic acid in water), applied over 30 min. The column was then washed with 90% mobile phase B before re-equilibrating at 3.2% mobile phase B.

Peptides were eluted directly (~350 nL/min) via a Triversa Nanomate nanospray source (Advion Biosciences, NY) into a QExactive HF Orbitrap mass spectrometer (Thermo Fisher Scientific). The spray voltage of QExactive HF was set to 1.7 kV through Triversa NanoMate and heated capillary at 275°C. The mass spectrometer performed a full MS scan (m/z 360–1600) and subsequent high energy collision dissociation (HCD) MS/MS scans of the 20 most abundant ions with dynamic exclusion setting 15S. Full scan mass spectra were recorded at a resolution of 120,000 at m/z 200 and an automated gain control (AGC) target of 3×10^6 . Precursor ions were fragmented in HCD MS/MS with the resolution set up at 15,000 and a normalized collision energy of 28. The AGC target for HCD MS/MS was 1×10^5 . The width of the precursor isolation window was 1.2 m/z and only multiply-charged precursor ions were selected for MS/MS. Spectra were acquired for 56 min.

The MS and MS/MS scans were searched against Uniprot database using Protein Discovery 2.2 software, Sequest HT algorithm (Thermo Fisher Scientific). Variable modifications were deamidation (N and Q), oxidation (M), phosphorylation (S, T and Y)

and acetylation (K). The precursor mass tolerance was 10 ppm and the MS/MS mass tolerance was 0.02 Da. Two missed cleavages were allowed and data was filtered with a false discovery rate (FDR) of 0.01. Proteins with at least two high-confidence peptides were accepted as a real hit. The software also calculated for each protein the abundance per sample, the median of the abundance per sample group (cell, sEV mock, sEV AcΔp6.9 or sEV AcMNPV), the ratio of abundance between samples (including the log₂ of the ratio), and both the regular and adjusted *p*-value of the abundance ratio. To calculate the adjusted *p*-value, the Benjamini–Hochberg method was used.

2.12 | Proteomics analysis

The proteomics data was returned by the University of Birmingham as a table of identified proteins, each with a list of peptides matching part of their sequence. Peptides that corresponded to a single protein were unique peptides. This data was further analysed using Rstudio (version 2022.12.0; <https://posit.co/products/open-source/rstudio/>). Proteins with only one or no unique peptide and those that were present in only one out of the three replicates were filtered out.

3 | RESULTS

3.1 | Characterisation of *S. frugiperda* sEVs

Small EVs were harvested from SfC1B5 cells grown in suspension culture by centrifugation followed by size exclusion chromatography (SEC)—a well-established technique (Davis et al., 2019; Taylor et al., 2011). Fractions of 0.5 mL were collected and analysed by NTA and BCA (Figure 1a). A peak of particles was observed between fractions 6–10, with sizes around 80–100 nm as is typical for sEVs (Figure 1b). The majority of proteins eluted from the column at fraction 13 onwards. The ratio between particles and proteins can provide an indication of the purity of an EV sample (Webber & Clayton, 2013). In this case, however, due to the high number of particles in the media, the assumption by Webber and Clayton (2013) that all particles are EVs was likely untrue. Therefore, the particle to protein ratio was not particularly informative here. A particle-rich fraction was observed by TEM, where characteristic cup-shaped vesicles were observed (Figure 1c).

Unfortunately, no marker proteins were known for sEVs released by *S. frugiperda*, therefore minimal information for studies of extracellular vesicles could not be fully provided (Théry et al., 2018). To study whether sEVs from AcMNPV-infected *S. frugiperda* cells incorporate baculovirus proteins, SEC was tested to separate sEVs from virions. However, qPCR analysis of elution fractions determined SEC was insufficient for this purpose (data not shown). Sucrose density gradient ultracentrifugation (SDGU) was suggested to enable separation (Alem et al., 2021; Bernardino et al., 2021; Ishikawa et al., 2020; Metz et al., 2013). However, despite excluding 95%–99% virions from fractions thought to be rich in EVs, no full separation was achieved using this method (data not shown). Therefore, a stable SfC1B5 cell line was generated producing viral glycoprotein GP64 (SfC1B5-GP64), to confirm the incorporation of GP64 into sEVs. Furthermore, Sf9 cells were transfected with the bacmid AcΔP6.9, to study sEVs in the absence of virions.

3.2 | GP64 is incorporated into sEVs released by SfC1B5-GP64

A plasmid harbouring the immediate early-2 promoter from OpMNPV expressing AcMNPV *gp64* was used to transfect SfC1B5 cells, to generate SfC1B5-GP64. GP64 production by this stable cell line was confirmed by Western blot (Figure 2a). Small EVs were harvested and presence of GP64 in these vesicles was also confirmed using the same method (Figure 2b). Compared to the amount in cells, GP64 was enriched in the sEVs.

To visualise the incorporation of GP64 into the sEV membrane, the vesicles were stained using immunogold and analysed by TEM. As a positive control baculovirus was included, which confirmed localisation of gold particles to GP64 (Figure 3a,b,d,e). Co-purified with baculovirus on the positive control were sEVs, which were stained with gold and therefore had incorporated GP64 (Figure 3c,f). Surprisingly, on the sEVs harvested from SfC1B5-GP64 cells, no GP64 was detected (Figure 3g–i).

To investigate a possible cause for this disparity, the levels of GP64 produced from infected cells were compared to that of SfC1B5-GP64 cells. GP64 production was considerably higher in infected cells, which may explain the apparent absence of GP64 detected by immunogold in SfC1B5-GP64 sEVs (Figure 4).

Ishikawa et al. (2020) used SDGU to separate baculovirus from sEVs, where virions migrated through the gradient while sEVs remained at the top. Here, GP64 acted as a marker protein for sEVs to confirm the localisation of sEVs following SDGU. Samples were taken throughout the isolation of sEVs. As expected, a strong GP64 signal was detected in pooled SEC fractions 6–10 (Figure 5a). Following SDGU, GP64 was detected only in the top fraction of the gradient, where sEVs were expected to remain (Figure 5b).

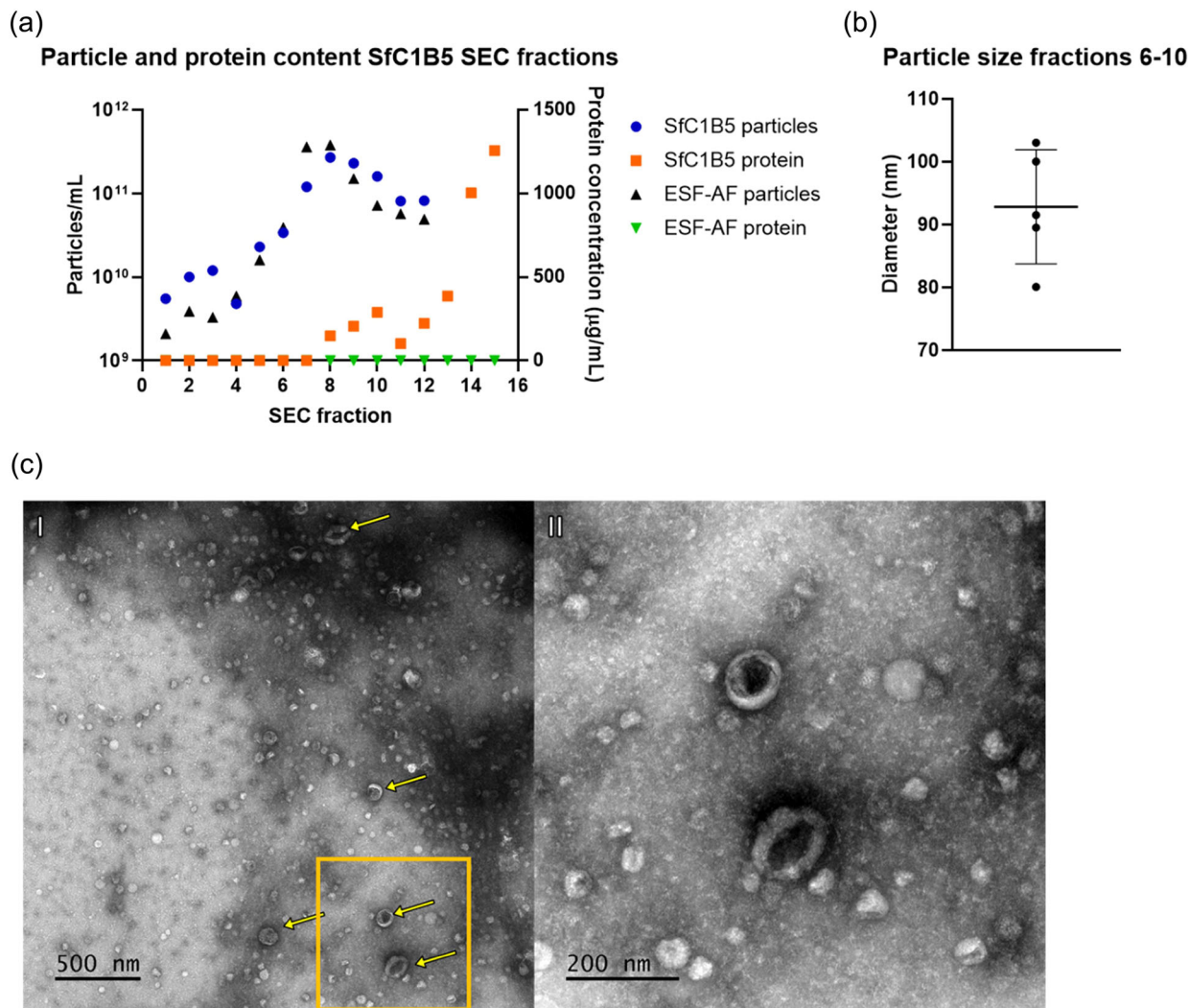


FIGURE 1 Characterisation of extracellular vesicle-like particles secreted by SfC1B5 cells. Particles were isolated from SfC1B5 culture medium and ESF-AF (70 mL each) by differential centrifugation at $300 \times g$ for 5 min and $16,500 \times g$ for 20 min, followed by concentration of the supernatant. The concentrated supernatant was further purified by SEC. Fractions of 0.5 mL were collected. The particle concentration of SEC fractions was determined by NTA (a, left Y-axis); the protein concentration was determined by BCA (a, right Y-axis). The NTA also determined the diameter of the most abundant particles in fractions 6–10 (b). Samples (10 μ L) of a particle rich fraction were applied on grids and incubated for approximately 2 min, before staining with 2% uranyl acetate. The samples were then imaged on the JEM-1400Flash microscope (Jeol). Representative images are shown (c). Arrows indicate extracellular vesicle-like structures. II is an enlargement of the box in I.

3.3 | Sf9 cells transfected with Ac Δ P6.9 secreted sEVs containing GP64

SfC1B5 cells were more resistant to transfection compared to Sf9 cells, therefore the latter were used here. Sf9 cells were transfected with Ac Δ P6.9, a modified AcMNPV genome unable to produce new virions, so that sEVs could be isolated in absence of virions. Transfected cells expressed GP64 on the plasma membrane, therefore the percentage of transfected cells was determined by flow cytometry using an anti-GP64 antibody conjugated to APC. Following optimisation, around 30% of cells were transfected (Figure 6a). Small EVs were harvested from the Ac Δ P6.9-transfected Sf9 cells and Western blot verified presence of GP64 in the vesicles (Figure 6b).

These small EVs from Ac Δ P6.9-transfected Sf9 cells were used to study the proteinaceous content, and to investigate the potential role of these vesicles in baculovirus infection, on the amount or timing of BV released. For the latter, Sf9 cells received sEVs as pre-treatment prior to AcMNPV infection. At various hours post infection (14–30) the culture medium was titrated for BV. No significant difference was observed between pre-treatment with sEVs derived from mock- or Ac Δ P6.9-transfected cells (data not shown).

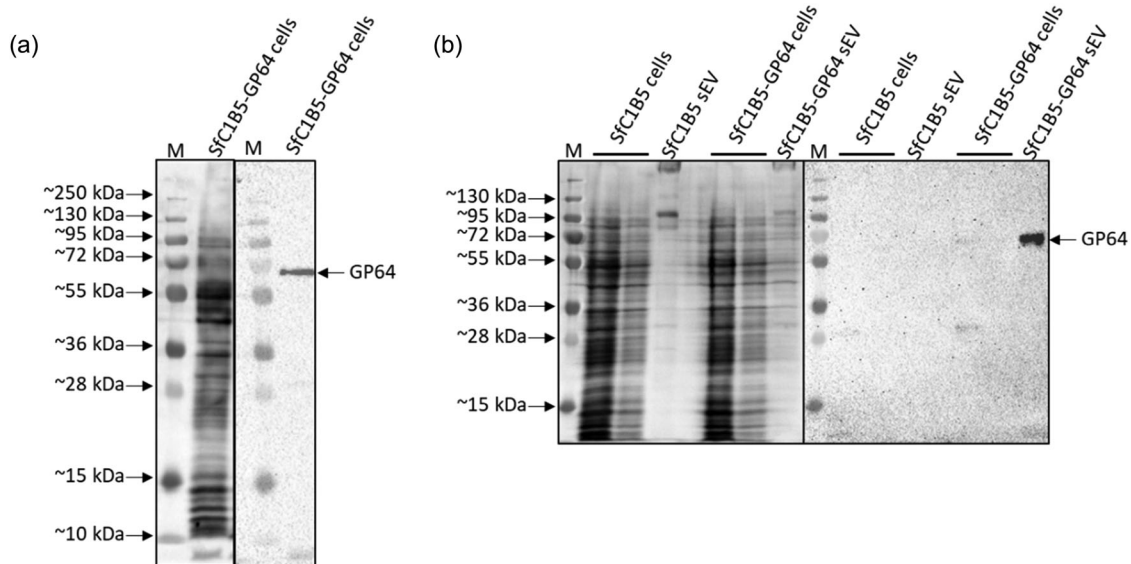


FIGURE 2 GP64 was produced in SfC1B5-GP64 stable cell line and enriched in sEVs. SfC1B5-GP64 cells were pelleted and used for Western blot (a). Small EVs were harvested from SfC1B5 and SfC1B5-GP64 culture medium (25 mL each) as described in Figure 1. Particle-rich fractions were pooled and concentrated, and GP64 production was compared to that of cells (b). The amount of protein was visualised using Revert™ 700 Total protein stain (left membranes). The membranes were probed with anti-GP64 AcV5 (right membranes).

3.4 | Proteomic analysis of sEVs from mock- and AcΔp6.9-transfected Sf9 cells

To gain information on protein content and abundance, three biological replicates of Sf9 cells ('cell'), sEVs from mock-transfected Sf9 cells ('sEV mock'), and sEVs from AcΔp6.9-transfected Sf9 cells ('sEV AcΔp6.9') were analysed by mass spectrometry. A protein was considered present when it was identified in at least two out of three replicates, and if it had at least two unique peptides. Knowing which proteins were enriched would provide valuable information, including suggestions for sEV marker proteins in *S. frugiperda*. The number of proteins identified in each sample and the overlap between samples are shown in Figure 7.

Of all the proteins, 732 were shared between the two sEV samples. Any protein in the sEV samples originates from the cells and should therefore be expected in the cell sample as well. Here, just 1 and 2 unique proteins were identified for sEV mock and sEV AcΔp6.9, respectively, and an additional 11 were shared between these two sEV samples but not cells. These proteins were likely present in the cell as well but below the detection limit. For sEV AcΔp6.9, the exceptions are viral proteins, but though there were four viral proteins detected (GP64, Ac-F, ME53 & viral ubiquitin), these were identified in the (non-transfected) cell sample as well—and in sEV mock for GP64 only. However, in cells and sEV mock these proteins were found at a much lower abundance.

GP64 was expected in the sEVs from AcΔp6.9-transfected cells, based on the observations above. Ac-F has a similar localisation and function to GP64, in other baculoviruses (granuloviruses and group II NPVs) (Lung et al., 2002). In AcMNPV, its function is different; it is not essential in BV budding or fusion with the plasma membrane, but instead accelerates the mortality rate (Lung et al., 2003; M. Wang et al., 2008). ME53 may be involved in packaging of structural components into the virion (de Jong et al., 2009). It is localised in the nucleus as well as the plasma membrane, where it co-localises with GP64, likely with the aid of other viral proteins (de Jong et al., 2011). Viral ubiquitin is slightly different from eukaryotic ubiquitin and has an extra lysine residue (Guarino, 1990; Negi et al., 2020). Ubiquitination via this alternative lysine is not well recognised by cellular deubiquitinases and protects the ubiquitin signal (Negi et al., 2020). Viral ubiquitination of the nucleocapsid is suggested to function as a signal for transport from the nucleus to the cytoplasm (Biswas et al., 2018).

3.5 | Significantly enriched proteins in sEVs from mock- and AcΔp6.9-transfected Sf9 cells

To visualise proteins enriched in sEV mock compared to cells, and therefore candidates for sEV marker proteins, a volcano plot was made. The thresholds set for significantly enriched proteins were a log₂ of fold change between sEV mock and cell of higher than 1 or lower than -1, and an adjusted *p*-value lower than 0.05. Five proteins were found to be significantly enriched in cells compared to sEV mock, while 50 were found to be significantly enriched in sEV mock compared to cells (Figure 8a).

The proteome of *S. frugiperda* cells is not well annotated yet, therefore the function of most proteins described here was inferred from homology (at least 90% similarity in amino acid sequence) or from conserved domains. An overview of all enriched proteins

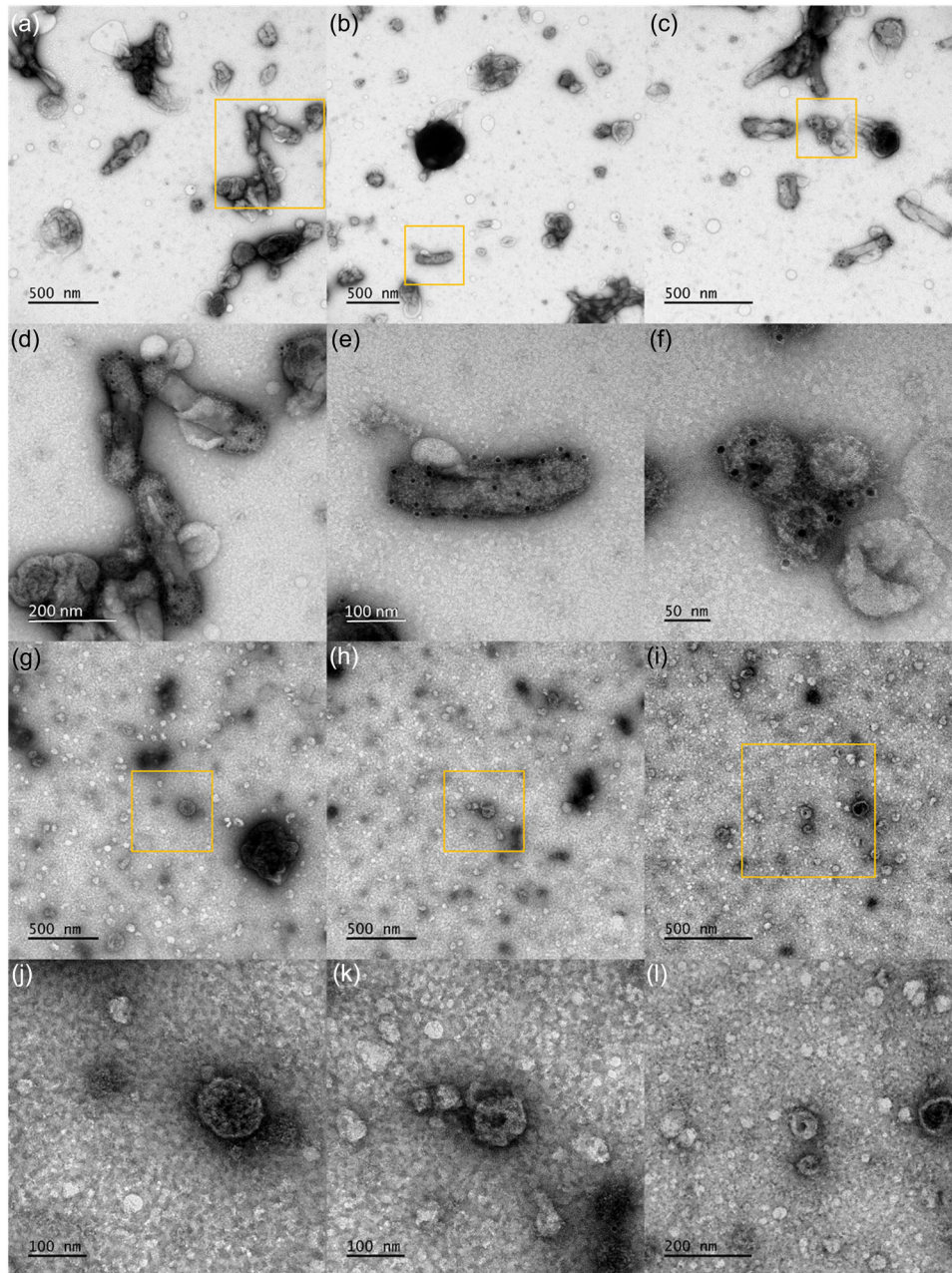


FIGURE 3 GP64 was detected on sEVs from AcMNPV-infected SfCIB5 cells but not on sEVs from SfCIB5-GP64 cells. Small EVs were harvested from SfCIB5-GP64 culture medium and wild-type (WT) AcMNPV-infected SfCIB5 culture medium (100 mL each) as described in Figure 1. Particle-rich SEC fractions were pooled and concentrated. Samples (10 μ L) were applied on grids and incubated for approximately 2 min. The samples were blocked with PBS-BSA (1%), stained with anti-GP64 AcV1 followed by anti-mouse-gold 10 nm and stained with 2% uranyl acetate. The samples were then imaged on the JEM-1400Flash microscope (Jeol). (a and b) AcMNPV budded virions. (c) Small EVs in AcMNPV sample. (d–f) Close-ups of (a–c), respectively. (g–i) Small EVs from SfCIB5-GP64 cells. (j–l) Close-ups of (g–i), respectively. Representative images are shown.

and their inferred functions is provided in Tables S1–S4. Interestingly, one of the proteins enriched in sEV mock compared to cells is TSG101, a protein of the ESCRT and a well-known marker for sEVs in mammalian cells. Two other proteins of the ESCRT were also identified. Furthermore, five identified proteins were likely part of laminin, a major component of the extracellular matrix and important in cell adhesion (Aumailley, 2013). Considering the size of laminins and its extracellular location, it was likely a contaminating artefact of the purification process. Finally, the G protein of Sf rhabdovirus was identified, highlighting the persistent infection of this virus in Sf9 cells (Ma et al., 2014).

A similar analysis was performed comparing the abundance of proteins between sEV mock and sEV Ac Δ p6.9, to examine the impact of baculovirus on the protein content of sEVs (Figure 8b). Forty proteins were significantly enriched in sEV mock

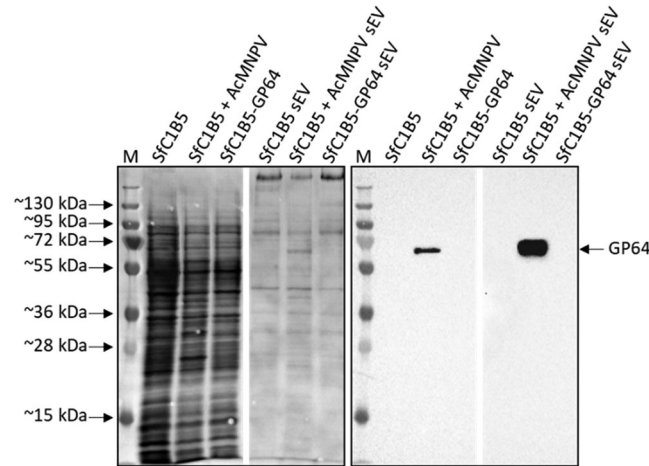
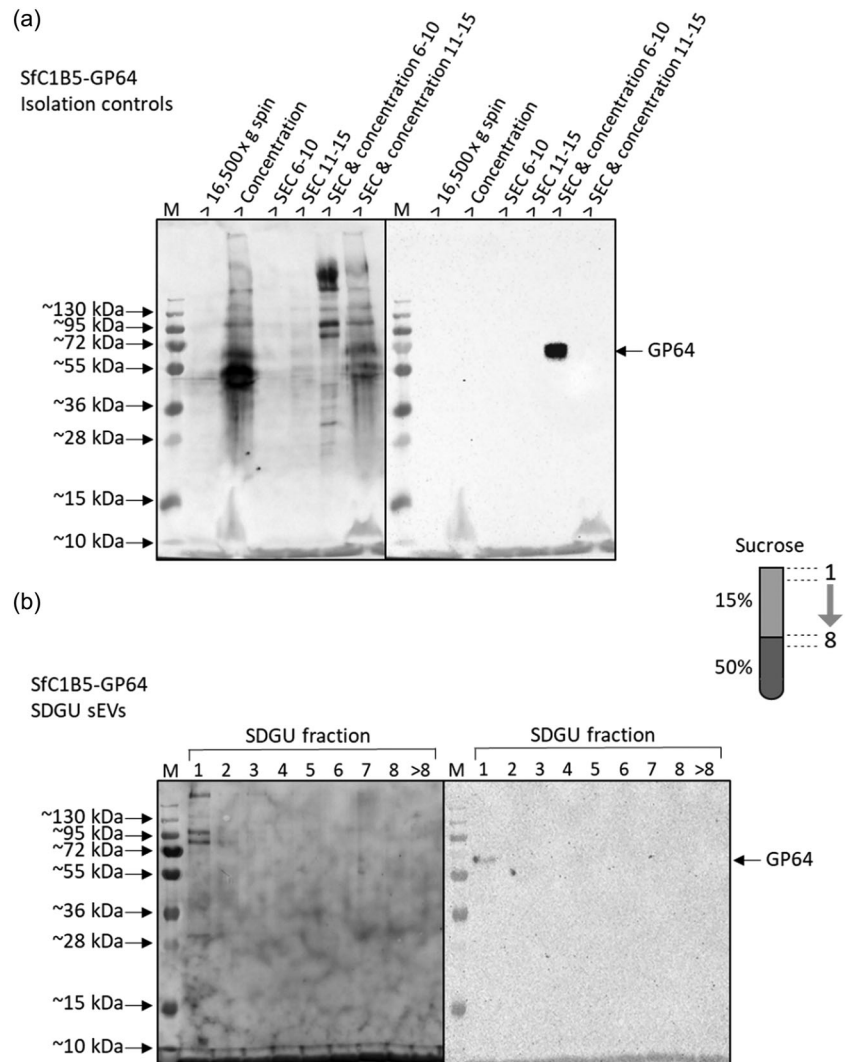


FIGURE 4 GP64 production was higher in infected cells compared to SfC1B5-GP64 cells. Cell pellets and sEVs were harvested from SfC1B5-GP64 and mock or WT AcMNPV-infected SfC1B5 culture medium (30 mL each) as described in Figure 1. Particle-rich fractions were pooled and concentrated. The amount of protein was visualised using Revert™ 700 Total protein stain (left membrane). The membrane was probed with anti-GP64 AcV5 (right membrane). Irrelevant lanes were omitted here, the full image is provided in Figure S4.

FIGURE 5 GP64 remained at top fraction following sucrose density gradient ultracentrifugation. Small EVs were harvested from SfC1B5-GP64 culture medium (200 mL) as described in Figure 1. Following SEC, particle-rich fractions 6–10 was pooled, as well as fractions 11–15 (protein-rich) and both were concentrated. They were applied on a 15%–50% sucrose gradient ($40,000 \times g$ for 1 h). Eight 1 mL fractions were collected from the top, with the rest of the gradient harvested as a single fraction. Samples taken throughout the isolation protocol were probed for GP64 (a), as well as the SDGU fractions of sEVs (b). The amount of protein in each sample was determined using Revert™ 700 Total protein stain (left membranes). ‘>’ indicates the sample was taken afterward, for example, ‘>concentration’ indicates the sample was taken directly after concentration.



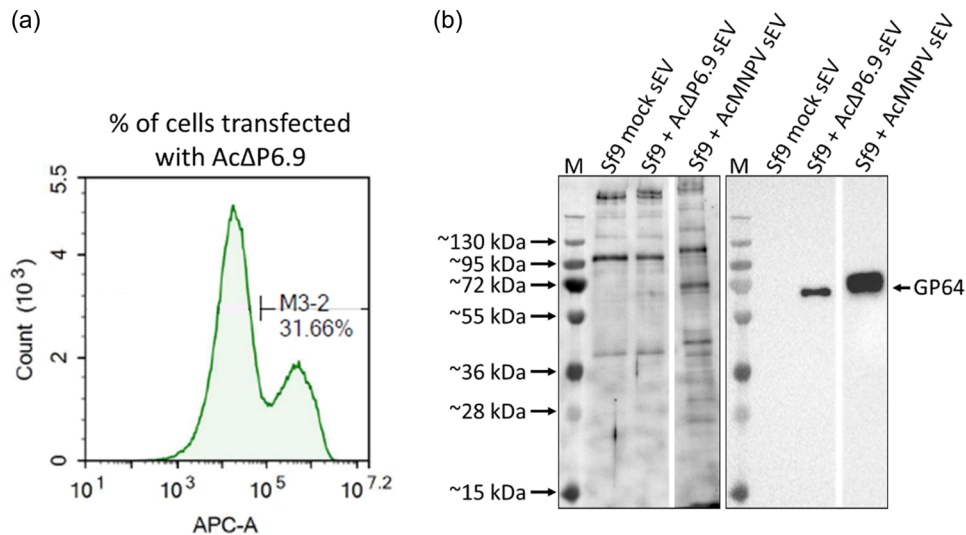


FIGURE 6 GP64 was present in sEVs harvested from cells transfected with AcΔP6.9. (a) Shake cultures (20 mL) of Sf9 cells were infected with WT AcMNPV at multiplicity of infection (MOI) 1, mock transfected, or transfected with AcΔP6.9. The following day three 0.5 mL samples per culture were harvested and cells were pelleted. The cells were stained with anti-GP64-APC and analysed by flow cytometry. The background signal of APC was determined using the mock cells and the transfection efficiency was measured for the transfected cells. Three replicates were analysed, and representative data is shown. (b) Small EVs were then harvested from these cultures as described in Figure 1. Particle rich fractions were pooled and concentrated, and used for Western blot. The amount of protein was visualised using Revert™ 700 Total protein stain (left membrane). The membrane was probed with anti-GP64 AcV5 (right membrane). Irrelevant lanes were omitted here, the full image is provided in Figure S5.

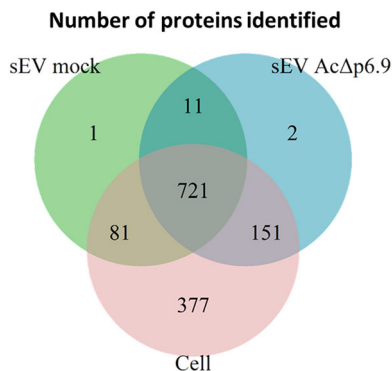


FIGURE 7 Number of proteins identified in Sf9 cells and sEVs isolated from mock- and AcΔp6.9- transfected Sf9 cells. Small EVs were harvested from mock-transfected and AcΔp6.9-transfected Sf9 cells, as described in Figure 1. Particle-rich SEC fractions were pooled and concentrated. Three biological replicates of Sf9 cells and sEVs were lysed, the proteins were digested with trypsin, and the peptides were identified by mass spectrometry.

compared to sEV AcΔp6.9, among which were a protein that may be Rab8a, two subunits of the eukaryotic translation initiation factor 3 (eIF-3) and two RNA helicases.

Rab8a is involved in transport between the trans-Golgi network, and the recycling endosome and plasma membrane (Hsu & Prekeris, 2010; Huber et al., 1993). It was also reported to be involved in the formation of primary cilia (Knödler et al., 2010). RNA helicases are involved in many processing steps of RNA; in transcription, translation, ribosome biogenesis and RNA degradation (Valentini & Linder, 2021). For only a few RNA helicases a specific function was discovered. eIF-3 is involved in translation, by stabilising the association between the 40S ribosomal subunit and Met-tRNA and subsequently mRNA. Upon association of the 60S ribosomal subunit, eIF-3 is released (Trachsel & Staehelin, 1979).

A further 142 proteins were significantly enriched in sEV AcΔp6.9 compared to sEV mock, among which were two proteins that may also be subunits of the eIF-3, two RNA helicases, four proteins relating to mitochondria, five proteins involved in ubiquitination, four proteins likely part of the proteasome complex, and 12 ribosomal proteins. Ubiquitination of a protein generally targets it for degradation by the proteasome complex (Hochstrasser, 1996). Furthermore, ubiquitination of a protein can direct its incorporation into intraluminal vesicles, and therefore to lysosomal degradation or secretion in exosomes (Velázquez-Cervantes et al., 2023).

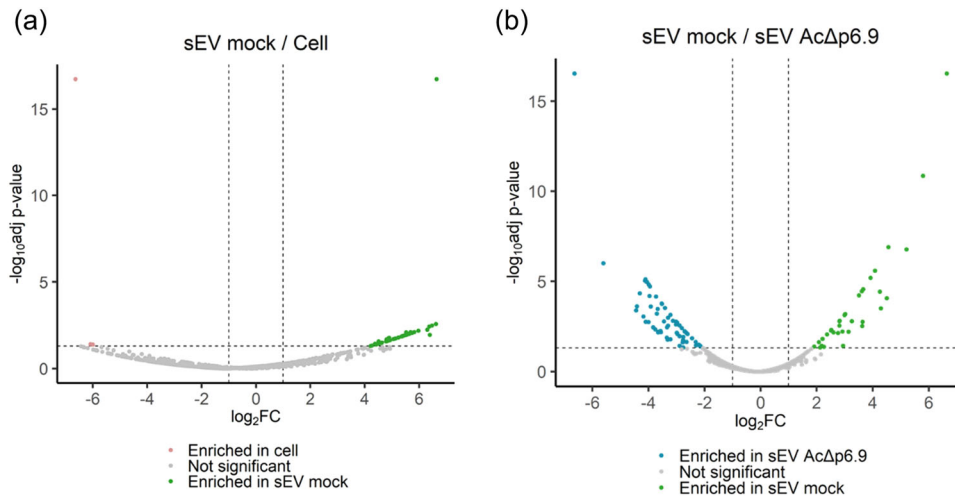


FIGURE 8 Volcano plots comparing enriched proteins in Sf9 cells with Sf9 sEVs (a), and Sf9 sEVs with sEVs from AcΔp6.9-transfected Sf9 cells (b). Small EVs were harvested from mock- and AcΔp6.9-transfected Sf9 cells, as described in Figure 1. Particle-rich SEC fractions were pooled and concentrated. Three biological replicates were lysed, 33 μg protein per replicate was digested with trypsin, and the peptides were identified by mass spectrometry. Relative abundances between the samples were compared, the \log_2 of fold change is represented on the X-axis. Significance is represented on the Y-axis as the -10 -log of the adjusted p -value. Proteins with a \log_2 of fold change greater than 1 or lower than -1 and an adjusted p -value of lower than 0.05 were considered significantly enriched.

4 | DISCUSSION

While EV secretion by *S. frugiperda* cells had been described previously, no characterisation of these EVs has yet been reported (Hashimoto et al., 2017; Ishikawa et al., 2020; Puente-Massaguer et al., 2022). Small EVs released by *Trichoplusia ni* cells during baculovirus infection were recently analysed by mass spectrometry, yet viral proteins were not analysed due to possible contamination by virions (Hausjell et al., 2023). To characterise sEVs of AcMNPV-infected cells, these vesicles had to be separated from the BV. Here, a stable cell line producing GP64 was first generated, to investigate incorporation of this viral glycoprotein into sEVs. It was confirmed to be present, and enriched in sEVs compared to the cells. Though immunogold TEM failed to detect GP64 on the surface of SfCIB5-GP64 sEVs, GP64 was detected on sEVs co-purified with baculovirus. An explanation for this discrepancy might be the fact that cells infected with baculovirus produced substantially more GP64 compared to SfCIB5-GP64 cells (Figure 4). Using this stable cell line, the expected localisation of sEVs following SDGU—at the top of the gradient (Ishikawa et al., 2020)—was confirmed.

For further characterisation of the vesicles during AcMNPV infection, AcΔP6.9 was used, as it was unable to produce new virions (Wang et al., 2010a). Detection of GP64 in sEVs from Sf9 cells transfected with AcΔP6.9 further consolidated the observation that GP64 was incorporated in Sf sEVs. One reason why GP64 was incorporated into sEVs might be to influence tropism. By incorporating GP64, the sEVs likely target the same cells as the BV and deliver their cargo to those cells that are susceptible to infection. Furthermore, GP64 is known to be fusogenic in acidic conditions (Blissard & Wenz, 1992). As such, the incorporation of GP64 in sEVs may increase the potential of back fusion of sEVs with endosomes following endocytosis, to release the cargo into the recipient cell (Tian et al., 2010). Alternatively, the incorporation of GP64 into sEVs may be simply due to its presence in endosomal membranes (Hodgson et al., 2022).

GP64 is localised to the plasma membrane of cells and was therefore expected to be incorporated into microvesicles (Volkman et al., 1984). In Figure 5a, the surprising observation was made that GP64 was incorporated into sEVs—thought to be mainly exosomes—but not mEVs—thought to be mainly microvesicles. Multiple explanations are possible for this. One is that the $16,500 \times g$ centrifugation step was not sufficient to pellet mEVs, and both were isolated together. This is considered unlikely since in previous studies centrifugation at $10,000$ – $16,500 \times g$ was sufficient to isolate mainly microvesicles (Heijnen et al., 1999; Jeppesen et al., 2019; Lischnig et al., 2022). Extracellular vesicles from *D. melanogaster* were reported to be smaller than vesicles from mammalian cells, on average (Lefebvre et al., 2016). Possibly, the microvesicles secreted by *S. frugiperda* were the size of sEVs. This is also considered unlikely, given the wide size range of microvesicles, from 100 – 1000 nm (Colombo et al., 2014). A faint but visible GP64 signal would have been expected in the concentrated mEVs in Figure 5a. Another possibility is that GP64 is secreted on exosomes due to its transport via the recycling endosome (Hodgson et al., 2022). Rather than being transported (back) to the plasma membrane following endocytosis, some of the GP64 may be secreted in exosomes via this endosome (Hodgson et al., 2022). However, this in itself would not exclude GP64 from being secreted via microvesicles. Perhaps the places in the plasma

membrane where baculovirus BV and microvesicles bud from have a different composition, and each particle only buds from its own 'place'. Alternatively, AcMNPV infection could inhibit microvesicle formation.

4.1 | Characterisation of the protein content of *S. frugiperda* sEVs

Proteomic analysis of the sEV mock sample revealed the presence of Sf rhabdovirus G protein in these vesicles. This was unsurprising since the Sf9 cell line is persistently infected with this virus (Ma et al., 2014). Regarding candidates for protein markers, TSG101 was identified. TSG101 is part of the ESCRT and considered a protein marker for sEVs from mammalian cells (Stuffers et al., 2009; Théry et al., 2001). Therefore, it is promising as a protein marker for sEVs of *S. frugiperda* cells. Charged multivesicular body protein 4 (or Snf7) and vacuolar protein sorting-associated protein 28 homolog (Vps28 homolog)—two other proteins of the ESCRT (Hurley, 2008)—were identified as well, providing further evidence that the ESCRT was involved in sEV biogenesis in *S. frugiperda* cells. Cross-reactivity of the antibody against mammalian TSG101 with that of *S. frugiperda* cells was not tested but would be most useful.

Rab proteins are involved in membrane trafficking within the cell and have specific localisations and functions (Homma et al., 2021). For example, Rab27 and Rab11 are involved in the release of sEVs, and were identified in proteomics (Jeon et al., 2021; Koles et al., 2012; Ostrowski et al., 2010; Théry et al., 2001). In sEV mock compared to cells, no Rab protein was enriched, however, a putative GTPase-activating protein was identified (Uniprot accession number A0A2H1VFN5). A GTPase-activating protein inactivates Rab proteins (Homma et al., 2021). The significance of this protein in sEVs is unclear.

In sEV AcΔp6.9, compared to sEV mock, 12 ribosomal proteins were found significantly enriched, as well as two RNA helicases and two proteins likely part of the eIF-3. All these proteins interact with RNA, suggesting its presence in these vesicles as well—as expected (Jeppesen et al., 2019; Noerholm et al., 2012; Willms et al., 2016). The incorporation of these components of the translation machinery into sEVs might simply reflect a change in cytosol composition. At the late stage of infection, replication of the baculovirus genome triggers a host protein shut-off, at the transcriptional level (Chen et al., 2014; Schultz & Friesen, 2009; Xue et al., 2012). Though the baculovirus is able to produce high levels of protein even after this shut-off, it is unclear whether the cell produces more translation machinery relative to mock-infected cells to facilitate this increase in protein production, which could then be reflected in the content of sEVs. Mitochondrial proteins were also found enriched in sEV AcΔp6.9. Baculovirus infection was reported to upregulate genes related to mitochondrial function and respiration (Chen et al., 2014; Xue et al., 2012). Therefore, enrichment of mitochondrial proteins in sEVs was likely a reflection of their upregulation, rather than selective incorporation of these proteins into the sEVs orchestrated by the baculovirus. A similar observation was made for proteins and genes of the proteasome complex (Xue et al., 2012).

Regarding the incorporation of viral proteins into sEVs, the possibility that under wild-type conditions P6.9 would be incorporated into sEVs cannot be excluded. It is, however, unlikely, considering this protein is localised in the nucleus and packaged into the viral capsid (Wang et al., 2010a). Considering its localisation in the plasma membrane, identification of Ac-F was also expected. Its significance in sEVs was not clear. During AcMNPV infection, Ac-F speeds up mortality (Lung et al., 2003), but it is not known whether it could trigger cell death by itself. ME53 was mainly considered a structural protein, though also reported to co-localise with GP64, explaining its presence. It was suggested to function as a matrix protein, connecting GP64 to the virus capsid (de Jong et al., 2011). Considering its function, it was not expected to have a significant effect on recipient cells. Last, the identification of viral ubiquitin suggested that one or multiple proteins (either cellular or viral) were ubiquitinated. The ubiquitinated proteins would likely be degraded via the proteasome in the recipient cell. Identification of only these four viral proteins, and not structural proteins such as vp39 or vp80, provided further confirmation that no BV—infectious or defective—were produced by AcΔp6.9-transfected cells.

Knowledge of which viral proteins are incorporated into sEVs can be helpful for research into VLP vaccine production with the baculovirus expression system. In a VLP vaccine for humans, BV is often considered a contaminating factor and it is depleted from the final product as much as possible (Pijlman, 2015). Based on the results described here, it can be recommended not to test for GP64 to confirm the absence of BV, since this may provide a false indication of BV presence. Instead, a structural protein such as VP39 is a better candidate to test for the presence or absence of BV (Lanier & Volkman, 1998).

Covert baculovirus infections of insects have been documented both in vivo and in vitro (Burden et al., 2003; Granados et al., 1978; Hughes et al., 1997). Moreover, some groups managed to establish a persistent baculovirus in cell culture (Baptista Arinto Garcia, 2019; Weng et al., 2009), including of AcMNPV in *S. frugiperda* (Crawford & Sheehan, 1983; Lee et al., 1998). A covert infection could provide an explanation for the observed presence of viral proteins in Sf9 cells by mass spectrometry here. If indeed the case, this covert infection is most likely a latent infection, rather than a persistent infection, considering only four viral proteins were detected, which were not sufficient to produce virions.

4.2 | Proteins not identified in *S. frugiperda* sEVs

In addition to identifying the viral proteins that were incorporated into sEVs, it was also interesting to discover those that were excluded. Viral structural proteins and those involved in the replication or transcription of DNA are localised to the nucleus and were therefore not expected to be incorporated into sEVs. In contrast, proteins localised to either cellular membranes or to the cytoplasm may be incorporated.

One viral protein of particular interest was P35. Due to its function in downregulating the antiviral response (Bump et al., 1995; Mehrabadi et al., 2015), it was anticipated to be incorporated into sEVs, to facilitate infection of neighbouring cells. Yet, mass spectrometry revealed it was not incorporated. A hypothesis for its exclusion is that P35 could inhibit an important step in the early stage of infection, such as cell entry, transport to the nucleus or nuclear entry. Transcription and translation are unlikely to be affected, since *p35* is expressed early in infection, and these processes are not inhibited (Chen et al., 2013). Furthermore, the baculovirus is known to prevent superinfection by additional virions (Crawford & Sheehan, 1983; Lee et al., 1998). P35, as well as other proteins not incorporated into sEVs, may be involved in this mechanism, and may therefore be excluded from sEVs.

No homologs of tetraspanins, other protein markers in mammalian sEVs (Potolicchio et al., 2005), were identified here. It is therefore likely that these sEVs were generated by a tetraspanin independent process. Alternatively, one or more of the proteins for which no function was inferred via homology or domains could be a tetraspanin. Another possibility is that *S. frugiperda* cells do not have or use the tetraspanin dependent process for sEV biogenesis at all—though identification of a tetraspanin in *D. melanogaster* sEVs suggests that the latter option is unlikely (Fradkin et al., 2002; Koles et al., 2012). An additional protein often identified in mammalian sEVs is syntenin-1, which is involved in ESCRT-dependent biogenesis of sEVs (Baietti et al., 2012; Kugeratski et al., 2021). A *S. frugiperda* protein enriched in both sEV mock and sEV AcΔp6.9 compared to cells (Uniprot accession number A0A2H1V4T0) may be a homolog of this protein, and therefore has potential to serve as a protein marker for sEVs as well.

A previous study on proteins associated with BV reported 11 *S. frugiperda* host proteins associated with BV (Wang et al., 2010b). Since the separation of BV and sEVs was challenging, it was possible that in their study, the host proteins were localised to sEVs instead of BV. Here, none of these 11 *S. frugiperda* host proteins were identified in the sEVs, suggesting that these proteins were indeed associated specifically with the BV.

5 | CONCLUSION

In conclusion, small EVs were released by *S. frugiperda* via the ESCRT-dependent pathway. No evidence of involvement of tetraspanins in the biogenesis of these vesicles was found. No Rab protein was found enriched in sEV mock compared to cell, therefore it was not clear which Rab was involved in vesicular transport. Baculovirus transfection affected the proteinaceous cargo of sEVs, compared to sEVs from mock-transfected Sf9 cells. Four viral proteins were incorporated into sEVs: GP64, Ac-F, ME53 and viral ubiquitin. In this study, the analysis focused on proteins with a function known or suspected based on homology or conserved domains. Future research could investigate in more detail the rest of the proteins identified here. The difference in abundance compared to the other samples may provide a first clue to their function.

AUTHOR CONTRIBUTIONS

Lex J. C. Van Es: Conceptualization (equal); data curation (equal); formal analysis (equal); methodology (equal); writing—original draft (equal). **Robert D. Possee:** Conceptualization (equal); formal analysis (equal); funding acquisition (equal); project administration (equal); supervision (equal); writing—review and editing (equal). **Linda A. King:** Conceptualization (equal); formal analysis (equal); funding acquisition (equal); project administration (equal); supervision (equal); writing—review and editing (equal).

ACKNOWLEDGEMENTS

We are thankful to Prof. Dave Carter (visiting Professor at Oxford Brookes University) and Dr. Ryan Pink for sharing their expertise relating to extracellular vesicles. We would also like to thank Dr. Flávia Moreira-Leite (Centre for Bioimaging, Oxford Brookes University) for her help with immunogold and regular transmission electron microscopy, and Dr. Leo Graves for his aid on the flow cytometry protocol. Lex J. C. Van Es was funded by a jointly funded Oxford Brookes University and Oxford Expression Technologies Ltd studentship.

CONFLICT OF INTEREST STATEMENT

The authors declare no conflicts of interest.

DATA AVAILABILITY STATEMENT

The mass spectrometry data used for this research is available at vesiclepedia (microvesicles.org; Study ID: 3593).

ORCID

Lex J. C. Van Es  <https://orcid.org/0009-0006-4987-2792>

REFERENCES

- Alem, F., Olanrewaju, A. A., Omole, S., Hobbs, H. E., Ahsan, N., Matulis, G., Brantner, C. A., Zhou, W., Petricoin, E. F., Liotta, L. A., Caputi, M., Bavari, S., Wu, Y., Kashanchi, F., & Hakami, R. M. (2021). Exosomes originating from infection with the cytoplasmic single-stranded RNA virus Rift Valley fever virus (RVFV) protect recipient cells by inducing RIG-I mediated IFN- β response that leads to activation of autophagy. *Cell & Bioscience*, 11(1), 220. <https://doi.org/10.1186/s13578-021-00732-z>
- Atkin-Smith, G. K., Tixeira, R., Paone, S., Mathivanan, S., Collins, C., Liem, M., Goodall, K. J., Ravichandran, K. S., Hulett, M. D., & Poon, I. K. H. (2015). A novel mechanism of generating extracellular vesicles during apoptosis via a beads-on-a-string membrane structure. *Nature Communications*, 6(1), 7439. Article 1. <https://doi.org/10.1038/ncomms8439>
- Aumailley, M. (2013). The laminin family. *Cell Adhesion & Migration*, 7(1), 48–55. <https://doi.org/10.4161/cam.22826>
- Ayres, M. D., Howard, S. C., Kuzio, J., Lopez-Ferber, M., & Possee, R. D. (1994). The complete DNA sequence of *Autographa californica* nuclear polyhedrosis virus. *Virology*, 202(2), 586–605. <https://doi.org/10.1006/viro.1994.1380>
- Baietti, M. F., Zhang, Z., Mortier, E., Melchior, A., Degeest, G., Geeraerts, A., Ivarsson, Y., Depoortere, F., Coomans, C., Vermeiren, E., Zimmermann, P., & David, G. (2012). Syndecan-syntenin-ALLX regulates the biogenesis of exosomes. *Nature Cell Biology*, 14(7), 677–685. Article 7. <https://doi.org/10.1038/ncb2502>
- Baptista Arinto Garcia, R. (2019). *Maintaining the balance: Persistent baculovirus infection in insect cells* [Ph.D., Oxford Brookes University]. <https://radar.brookes.ac.uk/radar/items/21b6bfa7-4800-4b89-99b3-8025644a8ffc/1/>
- Bernardino, T. C., Astray, R. M., Pereira, C. A., Boldorini, V. L., Antoniazzi, M. M., Jared, S. G. S., Núñez, E. G. F., & Jorge, S. A. C. (2021). Production of rabies VLPs in insect cells by two monoclonal baculoviruses approach. *Molecular Biotechnology*, 63(11), 1068–1080. <https://doi.org/10.1007/s12033-021-00366-z>
- Biswas, S., Willis, L. G., Fang, M., Nie, Y., & Theilmann, D. A. (2018). *Autographa californica* nucleopolyhedrovirus AC141 (Exon0), a potential E3 ubiquitin ligase, interacts with viral ubiquitin and AC66 to facilitate nucleocapsid egress. *Journal of Virology*, 92(3), e01713–e01717. <https://doi.org/10.1128/jvi.01713-17>
- Blissard, G. W., & Wenz, J. R. (1992). Baculovirus gp64 envelope glycoprotein is sufficient to mediate pH-dependent membrane fusion. *Journal of Virology*, 66(11), 6829–6835. <https://doi.org/10.1128/jvi.66.11.6829-6835.1992>
- Booth, A. M., Fang, Y., Fallon, J. K., Yang, J.-M., Hildreth, J. E. K., & Gould, S. J. (2006). Exosomes and HIV Gag bud from endosome-like domains of the T cell plasma membrane. *Journal of Cell Biology*, 172(6), 923–935. <https://doi.org/10.1083/jcb.200508014>
- Boucher, J., Rousseau, A., Boucher, C., Subra, C., Bazié, W. W., Hubert, A., Bourgeault, E., Benmoussa, A., Goyer, B., Tessier, P. A., & Gilbert, C. (2023). Immune cells release microRNA-155 enriched extracellular vesicles that promote HIV-1 infection. *Cells*, 12(3), 466. Article 3. <https://doi.org/10.3390/cells12030466>
- Bump, N. J., Hackett, M., Hugunin, M., Seshagiri, S., Brady, K., Chen, P., Ferenz, C., Franklin, S., Ghayur, T., Li, P., Licari, P., Mankovich, J., Shi, L., Greenberg, A. H., Miller, L. K., & Wong, W. W. (1995). Inhibition of ICE family proteases by baculovirus antiapoptotic protein p35. *Science*, 269(5232), 1885–1888. <https://doi.org/10.1126/science.7569933>
- Burden, J. P., Nixon, C. P., Hodgkinson, A. E., Possee, R. D., Sait, S. M., King, L. A., & Hails, R. S. (2003). Covert infections as a mechanism for long-term persistence of baculoviruses. *Ecology Letters*, 6(6), 524–531. <https://doi.org/10.1046/j.1461-0248.2003.00459.x>
- Campbell, T. D., Khan, M., Huang, M.-B., Bond, V. C., & Powell, M. D. (2008). HIV-1 Nef protein is secreted into vesicles that can fuse with target cells and virions. *Ethnicity & Disease*, 18, (2 Suppl 2), >S2–14–19.
- Chen, Y.-R., Zhong, S., Fei, Z., Gao, S., Zhang, S., Li, Z., Wang, P., & Blissard, G. W. (2014). Transcriptome responses of the host *trichoplusia ni* to infection by the baculovirus *Autographa californica* multiple nucleopolyhedrovirus. *Journal of Virology*, 88(23), 13781–13797. <https://doi.org/10.1128/jvi.02243-14>
- Chen, Y.-R., Zhong, S., Fei, Z., Hashimoto, Y., Xiang, J. Z., Zhang, S., & Blissard, G. W. (2013). The transcriptome of the baculovirus *Autographa californica* multiple nucleopolyhedrovirus in *Trichoplusia ni* cells. *Journal of Virology*, 87(11), 6391–6405. <https://doi.org/10.1128/jvi.00194-13>
- Cho, H. J., Velichkovska, M., Schurhoff, N., András, I. E., & Toborek, M. (2021). Extracellular vesicles regulate gap junction-mediated intercellular communication and HIV-1 infection of human neural progenitor cells. *Neurobiology of Disease*, 155, 105388. <https://doi.org/10.1016/j.nbd.2021.105388>
- Colombo, M., Raposo, G., & Théry, C. (2014). Biogenesis, secretion, and intercellular interactions of exosomes and other extracellular vesicles. *Annual Review of Cell and Developmental Biology*, 30, 255–289.
- Crawford, A., & Sheehan, C. (1983). Persistent baculovirus infections: *Spodoptera frugiperda* NPV and *Autographa californica* NPV in *Spodoptera frugiperda* cells. *Archives of Virology*, 78, 65–79.
- Davis, C. N., Phillips, H., Tomes, J. J., Swain, M. T., Wilkinson, T. J., Brophy, P. M., & Morphew, R. M. (2019). The importance of extracellular vesicle purification for downstream analysis: A comparison of differential centrifugation and size exclusion chromatography for helminth pathogens. *PLOS Neglected Tropical Diseases*, 13(2), e0007191. <https://doi.org/10.1371/journal.pntd.0007191>
- de Jong, J., Arif, B. M., Theilmann, D. A., & Krell, P. J. (2009). *Autographa californica* multiple nucleopolyhedrovirus me53 (ac140) is a nonessential gene required for efficient budded-virus production. *Journal of Virology*, 83(15), 7440–7448.
- de Jong, J., Theilmann, D. A., Arif, B. M., & Krell, P. J. (2011). Immediate-early protein ME53 forms foci and colocalizes with GP64 and the major capsid protein VP39 at the cell membranes of *Autographa californica* multiple nucleopolyhedrovirus-infected cells. *Journal of Virology*, 85(19), 9696–9707. <https://doi.org/10.1128/jvi.00833-11>
- Dogrammatzis, C., Saleh, S., Deighan, C., & Kalamvoki, M. (2021). Diverse populations of extracellular vesicles with opposite functions during herpes simplex virus 1 infection. *Journal of Virology*, 95(6), e02320–e02357. <https://doi.org/10.1128/jvi.02357-20>
- Fradkin, L. G., Kamphorst, J. T., DiAntonio, A., Goodman, C. S., & Noordermeer, J. N. (2002). Genomewide analysis of the *Drosophila* tetraspanins reveals a subset with similar function in the formation of the embryonic synapse. *Proceedings of the National Academy of Sciences*, 99(21), 13663–13668. <https://doi.org/10.1073/pnas.212511099>
- Granados, R. R., Nguyen, T., & Cato, B. (1978). An insect cell line persistently infected with a baculovirus-like particle. *Intervirology*, 10(5), 309–317. <https://doi.org/10.1159/000148993>
- Gruenberg, J. (2020). Life in the lumen: The multivesicular endosome. *Traffic (Copenhagen, Denmark)*, 21(1), 76–93. <https://doi.org/10.1111/tra.12715>
- Guarino, L. A. (1990). Identification of a viral gene encoding a ubiquitin-like protein. *Proceedings of the National Academy of Sciences*, 87(1), 409–413. <https://doi.org/10.1073/pnas.87.1.409>

- Hackenberg, M., Langenberger, D., Schwarz, A., Erhart, J., & Kotsyfakis, M. (2017). In silico target network analysis of de novo-discovered, tick saliva-specific microRNAs reveals important combinatorial effects in their interference with vertebrate host physiology. *Rna*, 23(8), 1259–1269. <https://doi.org/10.1261/rna.061168.117>
- Harrison, R. L., Herniou, E. A., Jehle, J. A., Theilmann, D. A., Burand, J. P., Becnel, J. J., Krell, P. J., van Oers, M. M., Mowery, J. D., & Bauchan, G. R., ICTV Report Consortium. (2018). ICTV virus taxonomy profile: Baculoviridae. *Journal of General Virology*, 99(9), 1185–1186. <https://doi.org/10.1099/jgv.0.001107>
- Hashimoto, Y., Macri, D., Srivastava, I., McPherson, C., Felberbaum, R., Post, P., & Cox, M. (2017). Complete study demonstrating the absence of rhabdovirus in a distinct Sf9 cell line. *PLoS ONE*, 12(4), e0175633. <https://doi.org/10.1371/journal.pone.0175633>
- Hausjell, C. S., Ernst, W., Grünwald-Gruber, C., Arcalis, E., & Grabherr, R. (2023). Quantitative proteomic analysis of extracellular vesicles in response to baculovirus infection of a *Trichoplusia ni* cell line. *PLoS ONE*, 18(1), e0281060. <https://doi.org/10.1371/journal.pone.0281060>
- Heijnen, H. F., Schiel, A. E., Fijnheer, R., Geuze, H. J., & Sixma, J. J. (1999). Activated platelets release two types of membrane vesicles: Microvesicles by surface shedding and exosomes derived from exocytosis of multivesicular bodies and -granules. *Blood, the Journal of the American Society of Hematology*, 94(11), 3791–3799.
- Hochstrasser, M. (1996). Ubiquitin-dependent protein degradation. *Annual Review of Genetics*, 30(1), 405–439. <https://doi.org/10.1146/annurev.genet.30.1.405>
- Hodgson, J. J., Buchon, N., & Blissard, G. W. (2022). Identification of cellular genes involved in baculovirus GP64 trafficking to the plasma membrane. *Journal of Virology*, 96(12), e00215–e00222. <https://doi.org/10.1128/jvi.00215-22>
- Homma, Y., Hiragi, S., & Fukuda, M. (2021). Rab family of small GTPases: An updated view on their regulation and functions. *The FEBS Journal*, 288(1), 36–55. <https://doi.org/10.1111/febs.15453>
- Hsu, V. W., & Prekeris, R. (2010). Transport at the recycling endosome. *Current Opinion in Cell Biology*, 22(4), 528–534. <https://doi.org/10.1016/j.ccb.2010.05.008>
- Huber, L. A., Pimplikar, S., Parton, R. G., Virta, H., Zerial, M., & Simons, K. (1993). Rab8, a small GTPase involved in vesicular traffic between the TGN and the basolateral plasma membrane. *Journal of Cell Biology*, 123(1), 35–45. <https://doi.org/10.1083/jcb.123.1.35>
- Hughes, D. S., Possee, R. D., & King, L. A. (1997). Evidence for the presence of a low-level, persistent baculovirus infection of *Mamestra brassicae* insects. *Journal of General Virology*, 78(7), 1801–1805. <https://doi.org/10.1099/0022-1317-78-7-1801>
- Hurley, J. H. (2008). ESCRT complexes and the biogenesis of multivesicular bodies. *Current Opinion in Cell Biology*, 20(1), 4–11. <https://doi.org/10.1016/j.ccb.2007.12.002>
- Ishikawa, R., Yoshida, S., Sawada, S., Sasaki, Y., & Akiyoshi, K. (2020). Preparation of engineered extracellular vesicles with full-length functional PD-1 membrane proteins by baculovirus expression system. *Biochemical and Biophysical Research Communications*, 526(4), 967–972. <https://doi.org/10.1016/j.bbrc.2020.03.187>
- Jeon, H., Kang, S.-K., Lee, M.-J., Park, C., Yoo, S.-M., Kang, Y. H., & Lee, M.-S. (2021). Rab27b regulates extracellular vesicle production in cells infected with Kaposi's sarcoma-associated herpesvirus to promote cell survival and persistent infection. *Journal of Microbiology*, 59(5), 522–529. <https://doi.org/10.1007/s12275-021-1108-6>
- Jeppesen, D. K., Fenix, A. M., Franklin, J. L., Higginbotham, J. N., Zhang, Q., Zimmerman, L. J., Liebler, D. C., Ping, J., Liu, Q., Evans, R., Fissell, W. H., Patton, J. G., Rome, L. H., Burnette, D. T., & Coffey, R. J. (2019). Reassessment of exosome composition. *Cell*, 177(2), 428–445. e18. <https://doi.org/10.1016/j.cell.2019.02.029>
- Knödler, A., Feng, S., Zhang, J., Zhang, X., Das, A., Peränen, J., & Guo, W. (2010). Coordination of Rab8 and Rab11 in primary ciliogenesis. *Proceedings of the National Academy of Sciences*, 107(14), 6346–6351. <https://doi.org/10.1073/pnas.1002401107>
- Koles, K., Nunnari, J., Korkut, C., Barria, R., Brewer, C., Li, Y., Leszyk, J., Zhang, B., & Budnik, V. (2012). Mechanism of evenness interrupted (Evi)-exosome release at synaptic boutons*. *Journal of Biological Chemistry*, 287(20), 16820–16834. <https://doi.org/10.1074/jbc.M112.342667>
- Koppen, T., Weckmann, A., Müller, S., Staubach, S., Bloch, W., Dohmen, R. J., & Schwientek, T. (2011). Proteomics analyses of microvesicles released by *Drosophila* Kc167 and S2 cells. *Proteomics*, 11(22), 4397–4410. <https://doi.org/10.1002/pmic.201000774>
- Kowal, J., Arras, G., Colombo, M., Jouve, M., Morath, J. P., Primdal-Bengtson, B., Dingli, F., Loew, D., Tkach, M., & Théry, C. (2016). Proteomic comparison defines novel markers to characterize heterogeneous populations of extracellular vesicle subtypes. *Proceedings of the National Academy of Sciences*, 113(8), E968–E977. <https://doi.org/10.1073/pnas.1521230113>
- Kugeratski, F. G., Hodge, K., Lilla, S., McAndrews, K. M., Zhou, X., Hwang, R. F., Zanivan, S., & Kalluri, R. (2021). Quantitative proteomics identifies the core proteome of exosomes with syntenin-1 as the highest abundant protein and a putative universal biomarker. *Nature Cell Biology*, 23(6), 631–641. Article 6. <https://doi.org/10.1038/s41556-021-00693-y>
- Lanier, L. M., & Volkman, L. E. (1998). Actin binding and nucleation by *Autographa californica* M Nucleopolyhedrovirus. *Virology*, 243(1), 167–177. <https://doi.org/10.1006/viro.1998.9065>
- Lee, J.-C., Chen, H.-H., & Chao, Y.-C. (1998). Persistent baculovirus infection results from deletion of the apoptotic suppressor gene p35. *Journal of Virology*, 72(11), 9157–9165. <https://doi.org/10.1128/jvi.72.11.9157-9165.1998>
- Lefebvre, F. A., Benoit Bouvrette, L. P., Perras, L., Blanchet-Cohen, A., Garnier, D., Rak, J., & Lécuyer, É. (2016). Comparative transcriptomic analysis of human and *Drosophila* extracellular vesicles. *Scientific Reports*, 6(1), 27680. Article 1. <https://doi.org/10.1038/srep27680>
- Lischnig, A., Bergqvist, M., Ochiya, T., & Lässer, C. (2022). Quantitative proteomics identifies proteins enriched in large and small extracellular vesicles. *Molecular & Cellular Proteomics*, 21(9), 100273. <https://doi.org/10.1016/j.mcpro.2022.100273>
- Lung, O., Westenberg, M., Vlask, J. M., Zuidema, D., & Blissard, G. W. (2002). Pseudotyping *Autographa californica* multicapsid nucleopolyhedrovirus (Ac M NPV): F proteins from group II NPVs are functionally analogous to Ac M NPV GP64. *Journal of Virology*, 76(11), 5729–5736.
- Lung, O. Y., Cruz-Alvarez, M., & Blissard, G. W. (2003). Ac23, an envelope fusion protein homolog in the baculovirus *Autographa californica* multicapsid nucleopolyhedrovirus, is a viral pathogenicity factor. *Journal of Virology*, 77(1), 328–339. <https://doi.org/10.1128/jvi.77.1.328-339.2003>
- Ma, H., Galvin, T. A., Glasner, D. R., Shaheduzzaman, S., & Khan, A. S. (2014). Identification of a novel rhabdovirus in *Spodoptera frugiperda* cell lines. *Journal of Virology*, 88(12), 6576–6585. <https://doi.org/10.1128/jvi.00780-14>
- Martínez-Rojas, P. P., Quiroz-García, E., Monroy-Martínez, V., Agredano-Moreno, L. T., Jiménez-García, L. F., & Ruiz-Ordaz, B. H. (2020). Participation of extracellular vesicles from Zika-virus-infected mosquito cells in the modification of naïve cells' behavior by mediating cell-to-cell transmission of viral elements. *Cells*, 9(1), 123. Article 1. <https://doi.org/10.3390/cells9010123>
- Martin-Jaular, L., Nevo, N., Schessner, J. P., Tkach, M., Jouve, M., Dingli, F., Loew, D., Witwer, K. W., Ostrowski, M., & Borner, G. H. (2021). Unbiased proteomic profiling of host cell extracellular vesicle composition and dynamics upon HIV-1 infection. *The EMBO Journal*, 40(8), e105492.
- Mehrabadi, M., Hussain, M., Matindoost, L., & Asgari, S. (2015). The baculovirus antiapoptotic p35 protein functions as an inhibitor of the host RNA interference antiviral response. *Journal of Virology*, 89(16), 8182–8192. <https://doi.org/10.1128/jvi.00802-15>
- Metz, S. W., Gardner, J., Geertsema, C., Le, T. T., Goh, L., Vlask, J. M., Suhrbier, A., & Pijlman, G. P. (2013). Effective Chikungunya virus-like particle vaccine produced in insect cells. *PLOS Neglected Tropical Diseases*, 7(3), e2124. <https://doi.org/10.1371/journal.pntd.0002124>
- Mulvania, T., Hayes, B., & Hedin, D. (2004). A flow cytometric assay for rapid, accurate determination of baculovirus titers. *BioProcessing Journal*, 3(3), 47.

- Negi, H., Reddy, P. P., Vengayil, V., Patole, C., Laxman, S., & Das, R. (2020). A novel polyubiquitin chain linkage formed by viral Ubiquitin is resistant to host deubiquitinating enzymes. *Biochemical Journal*, 477(12), 2193–2219. <https://doi.org/10.1042/BCJ20200289>
- Noerholm, M., Balaj, L., Limperg, T., Salehi, A., Zhu, L. D., Hochberg, F. H., Breakefield, X. O., Carter, B. S., & Skog, J. (2012). RNA expression patterns in serum microvesicles from patients with glioblastoma multiforme and controls. *BMC Cancer*, 12(1), 22. <https://doi.org/10.1186/1471-2407-12-22>
- Oliva Chávez, A. S., Wang, X., Marnin, L., Archer, N. K., Hammond, H. L., Carroll, E. E. M., Shaw, D. K., Tully, B. G., Buskirk, A. D., Ford, S. L., Butler, L. R., Shahi, P., Morozova, K., Clement, C. C., Lawres, L., Neal, A. J. O., Mamoun, C. B., Mason, K. L., Hobbs, B. E., ... Pedra, J. H. F. (2021). Tick extracellular vesicles enable arthropod feeding and promote distinct outcomes of bacterial infection. *Nature Communications*, 12(1), 3696. Article 1. <https://doi.org/10.1038/s41467-021-23900-8>
- Ostrowski, M., Carmo, N. B., Krumeich, S., Fanget, I., Raposo, G., Savina, A., Moita, C. F., Schauer, K., Hume, A. N., Freitas, R. P., Goud, B., Benaroch, P., Hachohen, N., Fukuda, M., Desnos, C., Seabra, M. C., Darchen, F., Amigorena, S., Moita, L. F., & Thery, C. (2010). Rab27a and Rab27b control different steps of the exosome secretion pathway. *Nature Cell Biology*, 12(1), 13–19. Article 1. <https://doi.org/10.1038/ncb2000>
- Parchure, A., Vyas, N., Ferguson, C., Parton, R. G., & Mayor, S. (2015). Oligomerization and endocytosis of Hedgehog is necessary for its efficient exovesicular secretion. *Molecular Biology of the Cell*, 26(25), 4700–4717. <https://doi.org/10.1091/mbc.E15-09-0671>
- Perrin, P., Janssen, L., Janssen, H., van den Broek, B., Voortman, L. M., van Elsland, D., Berlin, I., & Neefjes, J. (2021). Retrofusion of intraluminal MVB membranes parallels viral infection and coexists with exosome release. *Current Biology*, 31(17), 3884–3893.
- Pijlman, G. P. (2015). Enveloped virus-like particles as vaccines against pathogenic arboviruses. *Biotechnology Journal*, 10(5), 659–670.
- Posse, R. D. (1986). Cell-surface expression of influenza virus haemagglutinin in insect cells using a baculovirus vector. *Virus Research*, 5(1), 43–59. [https://doi.org/10.1016/0168-1702\(86\)90064-X](https://doi.org/10.1016/0168-1702(86)90064-X)
- Possee, R. D., Sun, T.-P., Howard, S. C., Ayres, M. D., Hill-Perkins, M., & Gearing, K. L. (1991). Nucleotide sequence of the *Autographa californica* nuclear polyhedrosis 9.4 kbp EcoRI-I and -R (Polyhedrin gene) region. *Virology*, 185(1), 229–241. [https://doi.org/10.1016/0042-6822\(91\)90770-C](https://doi.org/10.1016/0042-6822(91)90770-C)
- Potolicchio, I., Carven, G. J., Xu, X., Stipp, C., Riese, R. J., Stern, L. J., & Santambrogio, L. (2005). Proteomic analysis of microglia-derived exosomes: Metabolic role of the aminopeptidase CD13 in neuropeptide catabolism. *The Journal of Immunology*, 175(4), 2237–2243.
- Puente-Massaguer, E., González-Domínguez, I., Strobl, F., Grabherr, R., Striedner, G., Lecina, M., & Gòdia, F. (2022). Bioprocess characterization of virus-like particle production with the insect cell baculovirus expression system at nanoparticle level. *Journal of Chemical Technology & Biotechnology*, 97(9), 2456–2465.
- Reyes-Ruiz, J. M., Osuna-Ramos, J. F., De Jesús-González, L. A., Hurtado-Monzón, A. M., Farfan-Morales, C. N., Cervantes-Salazar, M., Bolaños, J., Cigarroa-Mayorga, O. E., Martín-Martínez, E. S., Medina, F., Fragoso-Soriano, R. J., Chávez-Munguía, B., Salas-Benito, J. S., & del Angel, R. M. (2019). Isolation and characterization of exosomes released from mosquito cells infected with dengue virus. *Virus Research*, 266, 1–14. <https://doi.org/10.1016/j.virusres.2019.03.015>
- Sambrook, J., & Russell, D. W. (2001). *Molecular cloning: A laboratory manual*. Cold Spring Harbor Laboratory Press.
- Sato, Y., Yaguchi, M., Okuno, Y., Ishimaru, H., Sagou, K., Ozaki, S., Suzuki, T., Inagaki, T., Umeda, M., Watanabe, T., Fujimuro, M., Murata, T., & Kimura, H. (2022). Epstein–Barr virus tegument protein BGLF2 in exosomes released from virus-producing cells facilitates de novo infection. *Cell Communication and Signaling*, 20(1), 95. <https://doi.org/10.1186/s12964-022-00902-7>
- Schultz, K. L. W., & Friesen, P. D. (2009). Baculovirus DNA replication-specific expression factors trigger apoptosis and shutoff of host protein synthesis during infection. *Journal of Virology*, 83(21), 11123–11132. <https://doi.org/10.1128/jvi.01199-09>
- Stuffers, S., Sem Wegner, C., Stenmark, H., & Brech, A. (2009). Multivesicular endosome biogenesis in the absence of ESCRTs. *Traffic (Copenhagen, Denmark)*, 10(7), 925–937. <https://doi.org/10.1111/j.1600-0854.2009.00920.x>
- Tassetto, M., Kunitomi, M., & Andino, R. (2017). Circulating immune cells mediate a systemic RNAi-based adaptive antiviral response in drosophila. *Cell*, 169(2), 314–325. e13. <https://doi.org/10.1016/j.cell.2017.03.033>
- Tauro, B. J., Greening, D. W., Mathias, R. A., Ji, H., Mathivanan, S., Scott, A. M., & Simpson, R. J. (2012). Comparison of ultracentrifugation, density gradient separation, and immunoaffinity capture methods for isolating human colon cancer cell line LIM1863-derived exosomes. *Methods (San Diego, Calif.)*, 56(2), 293–304. <https://doi.org/10.1016/j.jymeth.2012.01.002>
- Taylor, D. D., Zacharias, W., & Gercel-Taylor, C. (2011). Exosome isolation for proteomic analyses and RNA profiling. In R. J. Simpson, & D. W. Greening (Eds.), *Serum/plasma proteomics: Methods and protocols* (pp. 235–246). Humana Press. https://doi.org/10.1007/978-1-61779-068-3_15
- Théry, C., Bousiac, M., Véron, P., Ricciardi-Castagnoli, P., Raposo, G., Garin, J., & Amigorena, S. (2001). Proteomic analysis of dendritic cell-derived exosomes: A secreted subcellular compartment distinct from apoptotic vesicles. *The Journal of Immunology*, 166(12), 7309–7318.
- Théry, C., Witwer, K. W., Aikawa, E., Alcaraz, M. J., Anderson, J. D., Andriantsitohaina, R., Antoniou, A., Arab, T., Archer, F., Atkin-Smith, G. K., Ayre, D. C., Bach, J.-M., Bachurski, D., Baharvand, H., Balaj, L., Baldacchino, S., Bauer, N. N., Baxter, A. A., Bebawy, M., ... Zuba-Surma, E. K. (2018). Minimal information for studies of extracellular vesicles 2018 (MISEV2018): A position statement of the International Society for Extracellular Vesicles and update of the MISEV2014 guidelines. *Journal of Extracellular Vesicles*, 7(1), 1535750. <https://doi.org/10.1080/20013078.2018.1535750>
- Tian, T., Wang, Y., Wang, H., Zhu, Z., & Xiao, Z. (2010). Visualizing of the cellular uptake and intracellular trafficking of exosomes by live-cell microscopy. *Journal of Cellular Biochemistry*, 111(2), 488–496.
- Trachsel, H., & Staehelin, T. (1979). Initiation of mammalian protein synthesis. The multiple functions of the initiation factor eIF-3. *Biochimica Et Biophysica Acta (BBA)—Nucleic Acids and Protein Synthesis*, 565(2), 305–314. [https://doi.org/10.1016/0005-2787\(79\)90207-7](https://doi.org/10.1016/0005-2787(79)90207-7)
- Valentini, M., & Linder, P. (2021). Happy birthday: 30 years of RNA helicases. In M. Boudvillain, (Ed.), *RNA remodeling proteins: Methods and protocols* (pp. 17–34). Springer US. https://doi.org/10.1007/978-1-0716-0935-4_2
- Vaughn, J., Goodwin, R., Tompkins, G., & McCawley, P. (1977). The establishment of two cell lines from the insect *Spodoptera frugiperda* (Lepidoptera; Noctuidae). *In Vitro*, 13(4), 213–217.
- Velázquez-Cervantes, M. A., Benítez-Zeferino, Y. R., Flores-Pliego, A., Helguera-Repetto, A. C., Meza-Sánchez, D. E., Maravillas-Montero, J. L., León-Reyes, G., Mancilla-Ramírez, J., Cerna-Cortés, J. F., Baeza-Ramírez, M. I., & León-Juárez, M. (2023). A review study of the participation of late domains in sorting and transport of viral factors to exosomes. *Life*, 13(9), 1842. Article 9. <https://doi.org/10.3390/life13091842>
- Volkman, L. E., Goldsmith, P. A., Hess, R. T., & Faulkner, P. (1984). Neutralization of budded *Autographa californica* NPV by a monoclonal antibody: Identification of the target antigen. *Virology*, 133(2), 354–362. [https://doi.org/10.1016/0042-6822\(84\)90401-X](https://doi.org/10.1016/0042-6822(84)90401-X)
- Wang, M., Tan, Y., Yin, F., Deng, F., Vlask, J. M., Hu, Z., & Wang, H. (2008). The F-like protein Ac23 enhances the infectivity of the budded virus of gp64-null *Autographa californica* multinucleocapsid nucleopolyhedrovirus pseudotyped with baculovirus envelope fusion protein F. *Journal of Virology*, 82(19), 9800–9804. <https://doi.org/10.1128/jvi.00759-08>
- Wang, M., Tuladhar, E., Shen, S., Wang, H., van Oers, M. M., Vlask, J. M., & Westenberg, M. (2010a). Specificity of baculovirus P6.9 basic DNA-binding proteins and critical role of the C terminus in virion formation. *Journal of Virology*, 84(17), 8821–8828. <https://doi.org/10.1128/jvi.00072-10>
- Wang, R., Deng, F., Hou, D., Zhao, Y., Guo, L., Wang, H., & Hu, Z. (2010b). Proteomics of the *Autographa californica* nucleopolyhedrovirus budded virions. *Journal of Virology*, 84(14), 7233–7242. <https://doi.org/10.1128/jvi.00040-10>

- Webber, J., & Clayton, A. (2013). How pure are your vesicles? *Journal of Extracellular Vesicles*, 2(1), 19861. <https://doi.org/10.3402/jev.v2i0.19861>
- Weng, Q., Yang, K., Xiao, W., Yuan, M., Zhang, W., & Pang, Y. (2009). Establishment of an insect cell clone that harbours a partial baculoviral genome and is resistant to homologous virus infection. *Journal of General Virology*, 90(12), 2871–2876. <https://doi.org/10.1099/vir.0.013334-0>
- Willms, E., Johansson, H. J., Mäger, I., Lee, Y., Blomberg, K. E. M., Sadik, M., Alaarg, A., Smith, C. I. E., Lehtiö, J., EL Andaloussi, S., Wood, M. J. A., & Vader, P. (2016). Cells release subpopulations of exosomes with distinct molecular and biological properties. *Scientific Reports*, 6(1), 22519. Article 1. <https://doi.org/10.1038/srep22519>
- Xue, J., Qiao, N., Zhang, W., Cheng, R.-L., Zhang, X.-Q., Bao, Y.-Y., Xu, Y.-P., Gu, L.-Z., Han, J.-D. J., & Zhang, C.-X. (2012). Dynamic interactions between Bombyx mori nucleopolyhedrovirus and its host cells revealed by transcriptome analysis. *Journal of Virology*, 86(13), 7345–7359. <https://doi.org/10.1128/jvi.07217-12>
- Zhou, W., Tahir, F., Wang, J. C.-Y., Woodson, M., Sherman, M. B., Karim, S., Neelakanta, G., & Sultana, H. (2020). Discovery of exosomes from tick saliva and salivary glands reveals therapeutic roles for CXCL12 and IL-8 in wound healing at the tick–human skin interface. *Frontiers in Cell and Developmental Biology*, 8, 554. <https://www.frontiersin.org/articles/10.3389/fcell.2020.00554>

SUPPORTING INFORMATION

Additional supporting information can be found online in the Supporting Information section at the end of this article.

How to cite this article: Van Es, L. J. C., Possee, R. D., & King, L. A. (2024). Characterisation of extracellular vesicles in baculovirus infection of *Spodoptera frugiperda* cells. *Journal of Extracellular Biology*, 3, e163. <https://doi.org/10.1002/jex2.163>